



THE UPPER ATMOSPHERE OVER PERU

MARCH 2024



Several geomagnetic storms occurred in March 2024. On March 24th, a significant geomagnetic storm (G4-class) occurred with a Dst value of about -120 nT in the current solar cycle 25. The storm produced significant changes in the horizontal component of the geomagnetic field at Jicamarca and Piura. On the other hand, the X1.1 solar flare on March 28th produced D-layer absorption, as observed in ionograms recorded at the Jicamarca Radio Observatory (IGP-JRO), shown in [Figure 1](#).

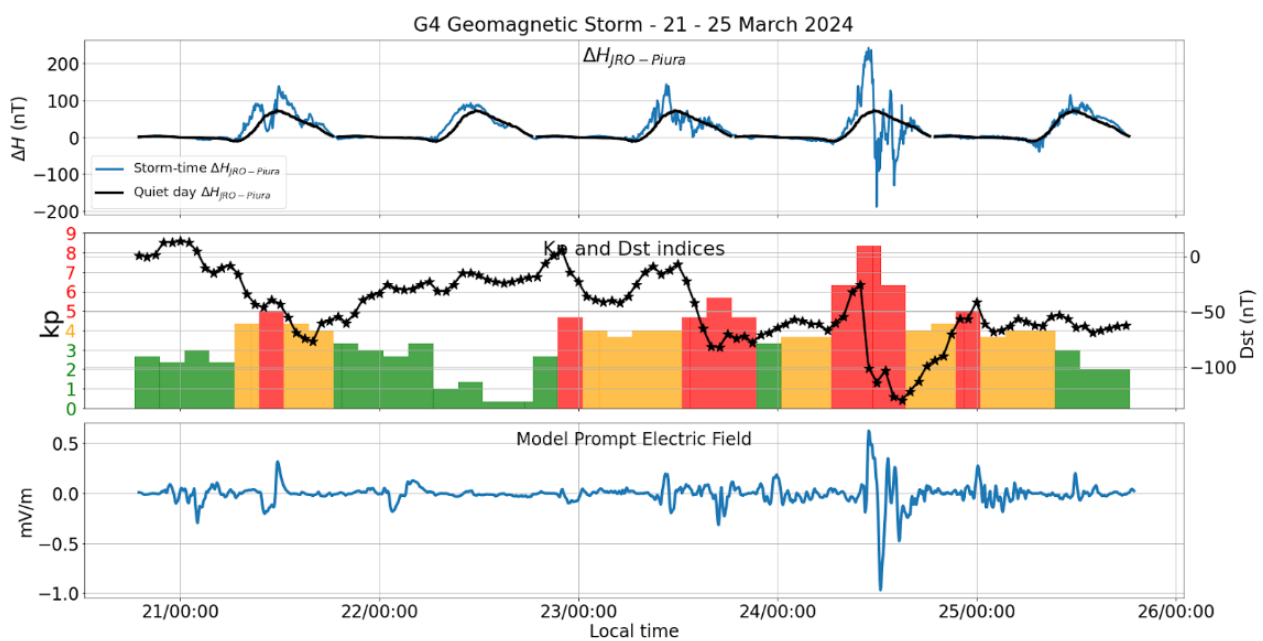


Figure 1. Geomagnetic conditions during the G4 class magnetic storm. The top panel shows variations on the H-component ($\Delta H_{ROJ-PIURA}$) at Jicamarca and Piura (blue curve) along with five international quiet days mean variation (black curve). The middle panel shows the k_p (bar plot) and Dst (black curve) indexes. The bottom panel shows the penetration electric field obtained from the model developed by the Cooperative Institute for Research in Environmental Sciences from the University of Colorado in Boulder[1].

Table 1. Summary of monthly measurements of ionospheric parameters and space weather predominant conditions. March 2024.

Average winds MLT at 90 km [m/s]		Maximum diurnal variation of the horizontal component of the geomagnetic field (H)[nT]		Average vertical plasma drifts (300 km- 400 km) [m/s]	
Meridional	Zonal	LIM:162	AQP:96	Min.	Max.
Min: 73.1 S	Min: 42.5 O	HYO: 159	NZC: 107	-37	35
Max: 34.4 N	Max: 11.6 E	PIU: 89			
GEOMAGNETIC ACTIVITY: QUIET			SOLAR ACTIVITY: MODERATE		

DID YOU KNOW THAT?

The prompt penetration electric field effect in the equatorial electric field refers to the quick transmission of the electric fields from high to lower latitudes to the equatorial ionosphere. This can happen with sudden polarity changes (positive to negative) of the Interplanetary Magnetic Field (IMF) and changes in solar wind conditions. Electric field disturbances caused by geomagnetic storms and magnetospheric substorms may affect the zonal electric field in the equatorial region. This can cause significant modifications in the electrodynamics of the equatorial ionosphere. This can cause considerable changes in the electrodynamics of the equatorial ionosphere. Figure 1 and Figure 4 demonstrate significant disturbances in equatorial electrojets (EEJ) (currents in the equatorial ionosphere). EEJ is calculated using equatorial and off-equatorial magnetometers ($EEJ = \Delta H_{ROJ} - \Delta H_{PIURA}$). Figure 1 shows that EEJ values were affected by electric field penetration during the abrupt polarity changes in the IMF Bz (Figure 2) between 14:30 and 16:00 UT on March 21. The disturbed zonal electric field plays an important role in the generation of plasma irregularities in the equatorial ionosphere during local nights, usually referred to as Equatorial Spread F

plasma irregularities. Even though these perturbations during the storms act globally, their impact may have longitudinal and stational dependencies. The zonal component of the electric field of the equatorial F region generally moves towards the west (east) during the night (day). For inactive geomagnetic conditions, this scenario remains unchanged except for the solstice of June during solar minimum years, when the zonal electric field of the F region changes strongly (based on statistical studies) towards the east near midnight.

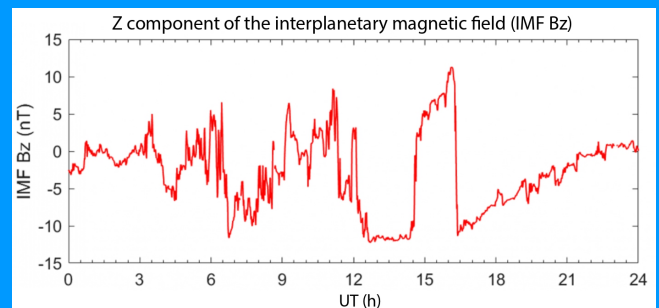


Figure 2. Perturbations of the Z component of the Interplanetary Magnetic Field (IMF Bz) during March 21st.

1. Climatology

The geomagnetic activity (Kp[2] index) was generally quiet 87% of the time, 8% moderate, and 5% strong; however, solar activity (F10.7[3]index) was high 42% of the time, and 58% moderate (see Figure 3 and Table 1, respectively). Previous studies have shown a significant relationship between the daily and seasonal variation of the horizontal component of the geomagnetic field (H)[4], something that we have verified with our observations too.

Spread-F is expected to occur more frequently before midnight, between 250 and 600 km, in months close to the March equinox, with high or moderate solar activity. However, few events are expected to take place after midnight. Previous measurements showed excellent agreement with climatology.

Compared to the Scherliess-Fejer model drift climatology for high or moderate solar activity, our measurements found F region plasma drift \sim 22 m/s after midnight and increased up at 10:00 UT, with a maximum value of 21 m/s. After that, it decreases to 8 m/s at 16:00 LT, then increases to 25 m/s at

18:00 UT because of the pre-reversal enhancement phenomena, just before decreasing to -25 m/s around midnight. The drift values estimated from the measurements are in moderate agreement with the climatology, except for the hours near the pre-reversal enhancement.

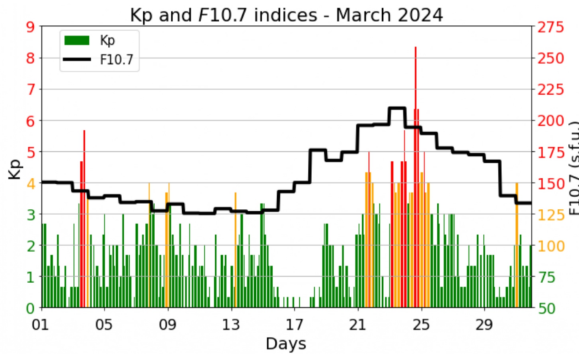


Figure 3. Kp and F10.7 cm(u.f.s. = $10^{-22} \text{Wm}^{-2} \text{Hz}^{-1}$) values for March, retrieved from OMNIWeb.

The March climatology (given by the Scherliess-Fejer model) for high or moderate solar activity, shows that the vertical plasma drift is ~ 22 m/s and increases to 21 m/s at an average height (300-400 km) after midnight. Following that, these values decrease to 8 m/s at 16:00 LT, then increase to 25 m/s at 18:00 LT due to the pre-reversal enhancement[5] phenomena, and then decrease to ~ 25 m/s before midnight.

Climatological studies[6] point out that for months close to the March equinox, the 150 km echoes appear around 9:00 LT, fade after 15:30 LT, and are detected between 140 and 165 km. During this period, we found that the minimum height of appearance of these echoes was lower by 10 km and that the maximum height of appearance was lower by approximately 5 km, while the time of appearance of these irregularities is consistent with the climatology.

2. Magnetic storms and solar flares

The increasing solar activity contributed to the occurrence of three of the most violent geomagnetic storms this year, which have caused disruptions in our magnetometer measurements. The first one occurred on March 3rd (Figure 4), with strength G2, and was initiated by a Coronal Mass Ejection (CME) that was expelled from the Sun on February 28. This ejection is accompanied by a C5.1 solar flare. The second, with strength G1, occurred on March 21st and was generated by a CME emitted on March 17th along with a class C5.1[7] solar flare. Finally, the third storm occurred between the 23rd and 25th of this month, with intensities G2, G4 and G1 respectively, being the most intense of the current solar cycle.

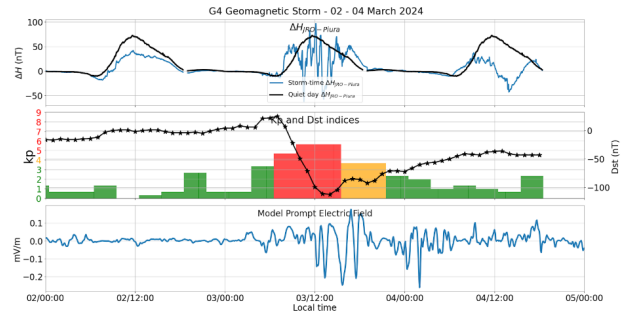


Figure 4. Geomagnetic conditions during the storm on March 3rd. The top panel shows $\Delta H_{ROJ-PIURA}$ values (magenta curve) for the storm days and along with the five quietest days of the month (black curve). In the middle panel: geomagnetic indexes Kp and Dst. The bottom panel displays the penetrating electric field obtained from the model developed by the Cooperative Institute for Research in Environmental Sciences from the University of Colorado in Boulder[1].

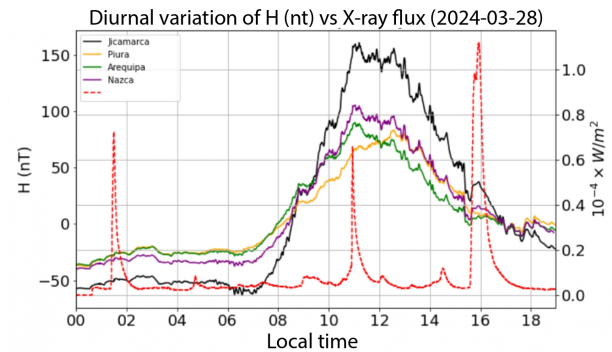


Figure 5. Magnetic crochet caused by a X1.1 class solar flare occurred on March 28th at 15:29 LT. This effect is more noticeable for stations closer to the magnetic equator.

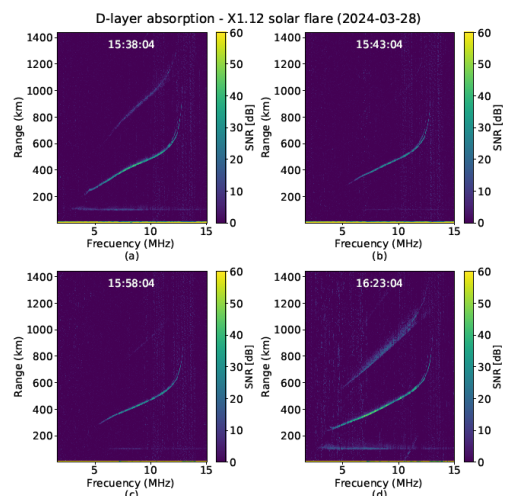


Figure 6. (a) Typical ionosonde echoes. (b) and (c) Temporary disappearance of the echoes detected by the ionosonde due to D-layer absorption caused by the X1.12 class solar flare on March 28th (d) Typical echo detection after the flare.

On the other hand, we observed two X1.1 solar flares. The first one occurred on March 23 at 8:32 p.m. local time, so we were unable to appreciate its effects. The second happened on March 28th at 15:29 LT, and it produced the appearance of extra currents, increasing the magnitude of the H-component in our magnetometers closer to the magnetic equator (Jicamarca, Huancayo, and Nazca). That resulted in a magnetic crochet[8], as seen in Figure 5. This flare contributed to the absorption of signals transmitted by the ionosonde[9], as shown in Figure 6.

3. Radar observations on the peruvian upper atmosphere

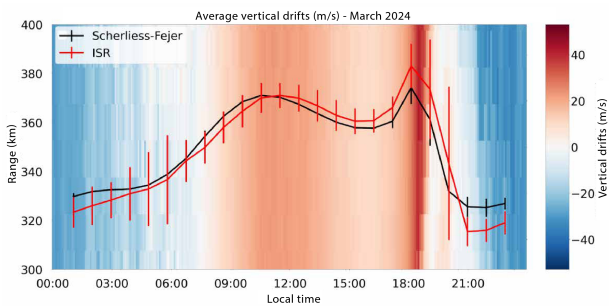


Figure 7. ISR average vertical drifts for March. The red curve represents the height average between 300 and 400 km and the black curve, the predicted values by the Scherliess-Fejer model.

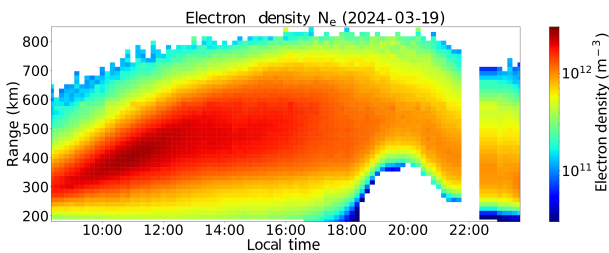


Figure 8. Electron density corresponding to March 15th.

The Jicamarca Radio Observatory’s main radar, part of the Instituto Geofísico del Perú (IGP-ROJ), measured the vertical plasma drift between 300 and 400 km using the JULIA-MP mode. These observations suggest that the average vertical drift went downward after midnight with values of -27 m/s and continued to increase until changing direction (upward) at 07:30LT. At 11:30 LT, it reached 22 m/s. Following that, the vertical drift decreased until a sharp rise around 18:00 LT, known as pre-reversal enhancement, with a value reaching 35 m/sec. Radar measurements show considerable agreement with Scherliess-Fejer model values, with a notable disagreement of around 13 m/s at 19:30 LT. In addition, the campaign to compare geophysical

data collected with the main radar with the AMISR-14 radar included estimates of the electron density of the F layer. Figure 8 shows a considerable increase in electron density ($\sim 2.62 \times 10^{12}$) on March 19th, around 11:00 LT.

On the other hand, 12 days of observations for the 150-km Echoes drifts were carried out to examine the transition region between the E and F layers. Figure 9 shows that echoes begin shortly before 09:00 LT, fade about 15:30 LT, and lay between 130 km and 165 km high, which is consistent with the climatology.

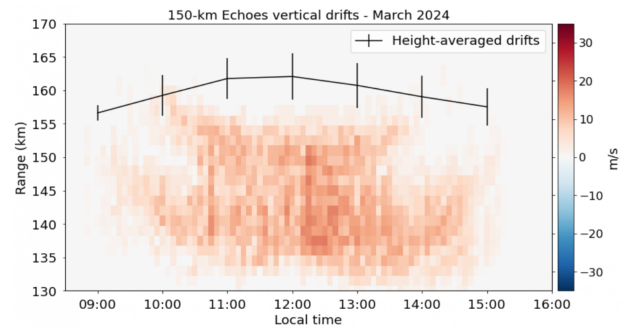


Figure 9. 150-km Echoes monthly average vertical drifts.

In addition, 22 nights of measurements were carried out with the AMISR-14[10] radar system. During this period, 16 F-layer irregularities happened during 16 nights at altitudes ranging from 200 km to 800 km. The dominant morphology was the Radar Plume type, with 63% occurrence, seconded by the Bottom-type and Bottom-side types, with 32% and 6%, respectively, as Figure 9 shows. These observations are consistent with the climatology results (performed with the main radar in JULIA mode)[11].

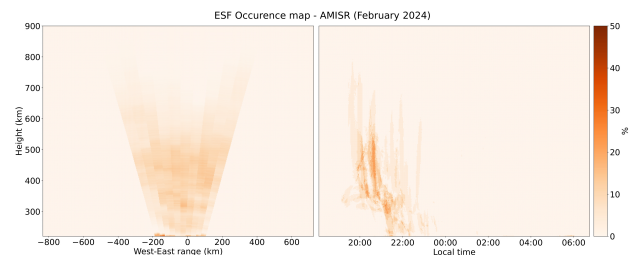


Figure 10. Right panel: traditional occurrence map. Left panel: polar occurrence map.

The time and height average of the zonal and meridional winds for March 2024 (see Figure 9) exhibit predominant periods of 24 hours (diurnal solar tide). In the mesopause (~ 90 km), we observed that the maximum value of the average zonal wind was +11.6 m/s at 13:30 LT, and the minimum average value was -42.5 m/s at 19:30 LT. The maximum average of meridional wind was +34.4 m/s at 17:00

LT, and the minimum average was -73.1 m/s at 02:30 LT. The maximum zonal wind was +97.1 m/s at 23:15 hours on March 8th, and the minimum -114.2 m/s at 23:15 LT on March 8th, while the maximum meridional wind was 143.1 m/s at 11:15 LT on March 27th, and the minimum -124.6 m/s.

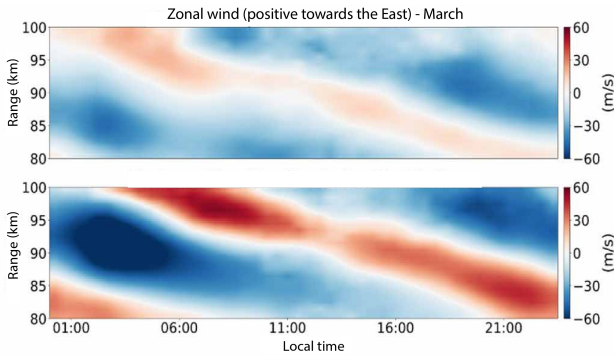


Figure 11. Monthly average zonal and meridional winds during March 2024.

4. LISN Observations

Figure 12 shows measurements of the horizontal component (H) of the geomagnetic field at the IGP-JRO magnetic stations. The average values of the Jicamarca and Huancayo stations were higher than the other locations because both magnetometers are located near the geomagnetic equator, and the enhanced Equatorial Electrojet (EEJ) contributes to an increase in their measurements. Furthermore, there was significant daily variability, particularly around 11:00 LT (16:00 UT). The maximum and minimum variations of the monthly average values for March are recorded for each station: Piura (89 nT), Huancayo (159 nT), Jicamarca (162 nT), Arequipa (96 nT), and Nazca (107 nT).

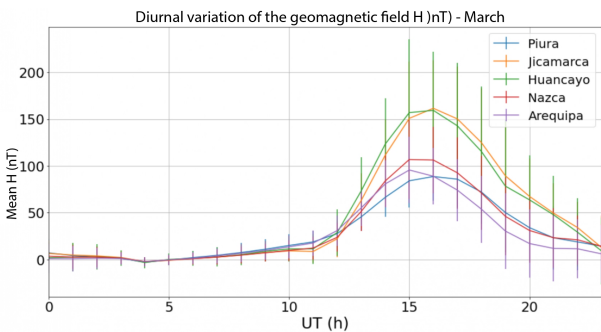


Figure 12. Hourly monthly average values of the diurnal variation of H-component for all of our magnetic stations operating during March 2024.

Figure 13 depicts amplitude scintillation index (S4) data from Jaén, Jicamarca, Catholic University of Peru,

and Cuzco stations. Our observations revealed levels of low, moderate, and high scintillation activity. The Cuzco Station reported the highest S4 index value of 1.3 at about 21:00 LT on March 1st.

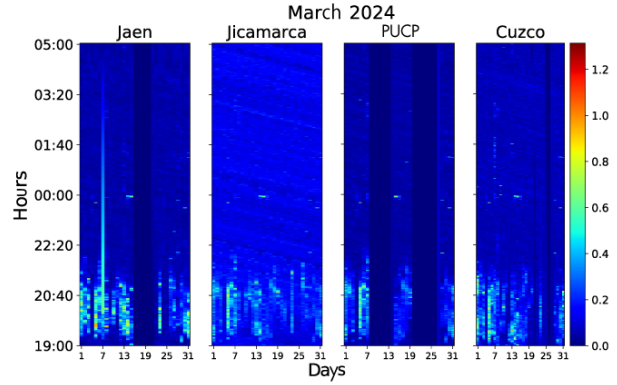


Figure 13. S4 maximum daily values for the Jaén, Jicamarca, Catholic University of Perú and Cuzco stations during March 2024. Low, moderate and high scintillation activity regimes were observed.

5. Conclusions

- We registered a high occurrence of geomagnetic storms that perturbed the geomagnetic field. That became evident with the magnetic field horizontal component difference of values between Jicamarca and Piura.
- We observed a D-layer absorption using the measurements obtained with the ionosonde. That is an effect of the class X1.1 solar flare.
- During the F layer density estimation campaign and using five days of measurements, we registered the highest density on March 19th at 11 LT with a value of 2.62×10^{12} .
- Low, moderate and high scintillation activities were reported. The highest value of 1.3 was registered at the Cuzco station on March 1st at 21:00 LT approximately.

6. References

[1] M. Williams, "Real-time model of the ionospheric electric fields - geomagnetism," <https://geomag.colorado.edu/real-time-model-of-the-ionospheric-electric-fields>.

[2] "The Kp-index | Help," Oct 2020, Accessed on: Feb. 01, 2023. [Online]. Available: <https://www.spaceweatherlive.com/en/help/the-kp-index.html>

- [3] "F10.7 cm Radio Emissions | NOAA / NWS Space Weather Prediction Center," Jul 2020, Accessed on: Feb. 01, 2023. [Online]. Available: [1https://www.swpc.noaa.gov/phenomena/f107-cm-radio-emissions](https://www.swpc.noaa.gov/phenomena/f107-cm-radio-emissions)
- [4] I. Adimula, K. Gidado, and S. Bello, "Variability of horizontal magnetic field intensity from some stations within the equatorial electrojet belt," *Physical Science International Journal*, vol. 13, pp. 1–8, 01 2017.
- [5] J. V. Eccles, J. P. St. Maurice, and R. W. Schunk, "Mechanisms underlying the pre-reversal enhancement of the vertical plasma drift in the low-latitude ionosphere." *J. Geophys. Res. Space Physics*, vol. 120, p. 4950–4970, 2015.
- [6] J. Chau and E. Kudeki, "Statistics of 150-km echoes over jicamarca based on low-power vhf observations," in *Annales Geophysicae*, vol. 24, no. 5. Copernicus GmbH, 2006, pp. 1305–1310.
- [7] "Cme impact sparks g2 - moderate geomagnetic storm.gnetism," <https://watchers.news/2024/03/04/cme-impact-sparks-g2-moderate-geomagnetic-storm>.
- [8] J. J. Curto, "Geomagnetic solar flare effects: a review. *J. Space Weather Space Clim*," 2020. [Online]. Available: [1doi:10,27.doi:10.1051/swsc/20200271](https://doi.org/10.1051/swsc/20200271)
- [9] "Instituto geofísico del Perú, "realtime at jicamarca," Mar. 2022, [Online; accessed 21. Mar. 2024]. [Online]. Available: [1https://www.igp.gob.pe/observatorios/radio-observatorio-jicamarca/realtime/static/reports/2022/Boletin_Marzo_2022.pdf](https://www.igp.gob.pe/observatorios/radio-observatorio-jicamarca/realtime/static/reports/2022/Boletin_Marzo_2022.pdf)
- [10] "Instituto Geofísico del Perú, "Realtime at Jicamarca," Aug. 2022, [Online; accessed 14. jan. 2024]. [Online]. Available: [1https://www.igp.gob.pe/observatorios/radio-observatorio-jicamarca/realtime/static/reports/2022/Boletin_Agosto.pdf](https://www.igp.gob.pe/observatorios/radio-observatorio-jicamarca/realtime/static/reports/2022/Boletin_Agosto.pdf)
- [11] W. Zhan, F. S. Rodrigues, and M. A. Milla, "On the genesis of postmidnight equatorial spread f: Results for the american/peruvian sector," *Geophysical Research Letters*, vol. 45, no. 15, pp. 7354–7361, 2018.

Developed by:

Bach. Roberto Flores Arroyo
Bach. Juan Pablo Velásquez Ormaeche

Design and layout:

Bach. Anette De la Cruz Meza

Collaborators:

Mag. Karim Kuyeng Ruiz
Dr. Danny Scipi3n Castillo
Mag. Luis Condori Illahuam3n
Dr. Edgardo Pacheco Josan
Dr. Marco Milla Bravo
Dr. Ram Singh

Contact:

roj@igp.gob.pe

Radio Observatorio de Jicamarca (ROJ)
Instituto Geofísico del Perú
Lurigancho-Chosica, Lima, Perú
Phone: +51 1 3172313
Webpage: www.gob.pe/igp

**"Ciencia para protegernos
ciencia para avanzar"**